CHAPTER

Nanomaterials in batteries 7

Baigang An[1,2], Han Zhang[1,2], Fang Di[1,2], Shuxin Li[1,2], Jingang Zheng[1,2], Lixiang Li[1,2]

[1]School of Chemical Engineering, University of Science and Technology Liaoning, Anshan, P.R. China; [2]Key Lab of Energy Materials and Electrochemistry Liaoning Province, University of Science and Technology Liaoning, Anshan, P.R. China

Over 30 years of development, lithium–ion batteries (LIBs) have been well applied in smart electronics, electric automobiles, and energy storage systems. Emerging Li–sulfur, metal–air, and all-solid-state batteries also demonstrate great promise for highly efficient energy storage systems. Nanotechnology-enabled materials played very important roles during these batteries' development and are promising in driving higher-performance batteries.

7.1 Nanomaterials in Li–ion batteries

In 1991, Sony released the first commercial LIB, which has achieved a large-scale application in smart electronics, electric vehicles, and power stations due to the advantages of high energy, stable working voltage, wide operating range, and good stability. Nanomaterials have made vital contributions with the updating technology requirements for the improved performance of LIBs.

7.1.1 Avoid side reactions on the electrode

As a material most used in anode of LIBs, energy storage is accomplished by intercalating lithium ions into the graphite interlayer: $6\,C + xLi^+ + xe^- \rightarrow Li_xC_6$ ($0<x<1$), resulting in the lithium storage capacity of 372 mAh/g. The advantage is that the graphite crystal structure is maintained during the lithium storage process; thus, the graphite has good cycle stability. However, side reactions during graphite lithiation limit its further development. For example, graphite undergoes irreversible side reactions with commonly used organic electrolytes. Although the byproduct does not affect Li^+ transfer, it can cause the exfoliation of graphite sheets and the reduction/decomposition of electrolytes. Therefore, strategies have been developed to protect the graphite anodes [1]. Nano-coatings are effective ways to block the side reactions between graphite and electrolyte. Amorphous carbon, metal/metal oxides, and polymers commonly use nano-coatings. Amorphous car-

Handbook of Nanomaterials, Volume 1. https://doi.org/10.1016/B978-0-323-95511-9.00025-1

bon coating is typically deposited using the organic and polymer as precursors by thermal vapor deposition (TVD) and high-temperature annealing in an inert atmosphere. Constructing a metal or metal oxide coating with a nanoscale thickness onto the graphite can also effectively reduce side reactions to enhance the rate performance of the anode [2–4].

$LiNi_{1-x-y}Mn_xCo_yO_2$ ($0 \leq x, y, x+y \leq 0.5$ NMC) is a widely used cathode material and can supply about 200 mAh/g capacity [5]. Because of the substantial mixing between the 3d orbit of Ni and the 2p orbit of oxygen, the delithiated Ni-rich cathode suffers the side reaction in nonaqueous electrolytes that leads to the battery capacity drop, interface resistance increases, and battery safety decline. Several protective strategies have been reported to prevent Ni-rich cathodes from adverse reactions [6,7]. In general, a chemically inert nano-coating can block the side reactions, enabling the cathode to have good cycle stability. The coatings typically consist of various oxides, fluoride, or phosphate with a particle size of 5~20 nm. The core–shell nanostructure of Ni-rich cores and Mn-rich shells is another good strategy. Compared with the Ni-rich counterpart, the Mn-rich phase has a lower capacity but better interfacial stability in nonaqueous electrolytes. Core–shell separation during cycling due to the lattice characteristic of the materials is a major challenge limiting this strategy. The core–shell structures with the nano-functional full-gradient have been developed to eliminate the mismatch of the lattice parameters between the core and shell. The Ni concentration decreases gradually from the inner core to the outer shell. Meanwhile, the Mn concentration gradually increases [8]. The full-gradient approach through nanotechnology shows that the Ni-rich core has high-energy density and that the Mn-rich outer layer has high thermal stability. Moreover, the aligned needle-like nanoparticles assure the cathode has an excellent rate performance. In a full cell test, the material with nano-functional full-gradient can deliver 200 mAh/g capacity and good cycling stability.

7.1.2 Improve electron/ion transport path

A good conductive network for electrons and the short distance of ions transport are necessary conditions for electrode materials with high-rate performance. Nanomaterials can shorten the transport of ions and electrons compared to micronized materials.

Nanostructured $LiFePO_4$ has been successfully constructed to pave the way for its application in hybrid electric vehicles (HEVs) and electric vehicles (EVs). Because $LiFePO_4$ has significantly higher-power density, longer service life, and higher safety than $LiCoO_2$, it has been widely used in energy storage systems. Related studies have confirmed that the polyanionic framework in $LiFePO_4$ restricts the conductivity. Nanosized $LiFePO_4$ can effectively reduce the electron transport length. Another factor limiting the kinetic performance of $LiFePO_4$ is the poor percolation properties in its one-dimensional diffusion channels. The diffusion coefficient of Li^+ along the (010) direction in one-dimensional channels was obtained by Ab initio calculations, suggesting that the Fe ions occupation in Li sites (antisite de-

fects) can prevent Li^+ from hopping through the crystal structure [9]. In addition, the diffusion of Li^+ along the (001) direction is significantly delayed to block Li diffusion, resulting in a large electrochemical polarization and worse rate performance. Therefore when the $LiFePO_4$ is decreased to a critical value, the number of trapped Li ions can be significantly reduced.

7.1.3 Inhibit electrode cracking and powdering

The intercalation-type materials such as graphite have small volume changes (<10%) since the lattice characteristic is not changed during the lithium ions intercalation. The alloy-type materials generally own a significantly larger Li ions storage capacity than the graphite anode. As the typical alloy anode, silicon has a capacity of 3579 mAh/g for Li ions storage; however, Si suffers a large volume change of 420% during (de)lithiation causing the rapid capacity loss of LIBs. The mechanical stress resulting from volumetric change is the vital factor limiting the application of alloy-type anode material of Ge and Sn by 260% and P by 300% in the volumetric changes (Fig. 7.1A) [10]. The mechanical stress induced by these significant volume changes results in mechanical failures, such as material fracture, pulverization, and separation from the current collectors, significantly shortening the cycle life.

Nanomaterials can alleviate volume expansion and resist the mechanical failure of the electrode. The critical fracture size of electrode materials depends on the ma-

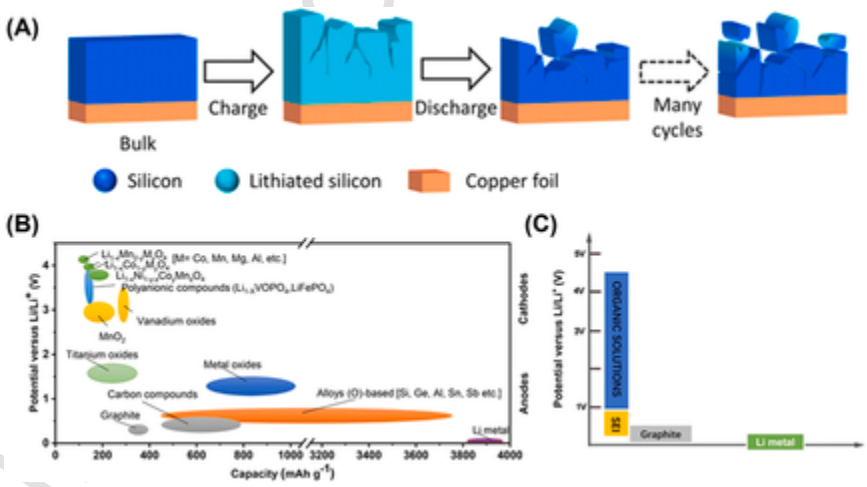

FIGURE 7.1

(A) Cracking and fracture of alloy-type active particles over lithiation/delithiation cycling [10]. Copyright 2017, Reproduced with permission of American Chemical Society. (B) Voltage versus capacity for cathodic and anodic materials. (C) The voltage windows for electrolyte stability and the formed SEI.

terial's lithiation mechanism, physical properties, and volumetric change ratio. The mechanism of stress generation, particle mechanical failure, and the reasonable size of Si particles were systematically studied by TEM. A particle smaller than 150 nm can accommodate the strain caused by lithiation to avoid particle cracking or pulverization [11].

One-dimensional silicon nanomaterials (Si nanowires, Si nanotubes) have better structural stability due to their good mechanical properties [12,13]. Since the reaction occurs at the interface between the electrode and electrolyte, one-dimensional nanomaterials can increase the electrochemical reaction sites due to the larger specific surface area. In terms of mass transport, the axial one-dimensional nanomaterials facilitate the transfer of ions to enhance the reaction kinetics. Furthermore, nanotubes are more efficient in alleviating volumetric stress than nanowires owing to the hollow space of the inner tube.

7.1.4 Generation of stable solid electrolyte interfaces

Since the electrochemical working voltage of the anode is lower than the voltage that the organic carbonate solvent in common organic electrolytes is reduced (about 1.0 V vs Li^+/Li), the electrolyte undergoes a reduction reaction during the charging to produce a solid electrolyte interlayer (SEI) is on the surface of anode materials (Fig. 7.1B and C) [14]. Although SEI is a Li^+ conductor relative to electronic insulation, the growth of SEI consumes electrolytes and hinders the migration of ions and electrons. Therefore a stable SEI layer is highly expected for the rate capability and stability of the anode. Unfortunately, stable SEI films are not easy to obtain in high-capacity lithium and silicon anodes.

The extremely low reduction potential of metallic lithium leads to the inevitable reaction between itself and the electrolyte, and the heterogeneous SEI is easily broken during the charge–discharge cycles [15]. The stable SEI film is necessary for improving the electrochemical reversibility and stability of the lithium metal anode. The current research mainly focuses on electrolyte optimization and artificial nano SEI construction. Compared with electrolyte optimization, artificial nano SEI construction can more efficiently improve the long-cycle performance of lithium anode. An SEI film with a specific composition can be formed through the reaction between metallic lithium and an initiator. It was found that reactive gases can passivate the negative electrode to a certain extent. Freon can also react with graphene composite and metal lithium anode to form an effective LiF interface. With the continuous exploration of the compositional structure of SEI, a lithiophilic/lithiphobic gradient interface layer (ZnO/CNT-CNT) can better realize the lithium deposition under the protective layer, thereby ensuring the ultra-long cycling of lithium metal anodes [16].

Another example of an unstable SEI is the silicon anode, which ruptures and restructures due to repeated volume changes. The disadvantages of unstable SEI mainly cause the low capacity and power reduction of LIBs. Therefore Wu et al. [17] designed an SEI around silicon nanotubes because the hollow space of nan-

otubes can provide the necessary voids to accommodate the volume expansion. Recently, to inhibit the volumetric expansion of Si lithiation, the tough TiO_2, SiC, SiO_x, and TiO_x were used as shells to protect structural Si during cycles [18–21].

7.2 Nanomaterials in Li–S batteries

Lithium-sulfur (Li–S) battery was investigated since the 1960s. Since the commercialization of LIBs, no breakthroughs have been made in solving the fatal problems facing Li–S batteries for many years. Since 2009, it has got more concerns as an excellent candidate for the next generation of high-efficiency electrical energy storage technologies after the revolutionary technology of Li–S battery with improved performance [22]. By matching the sulfur cathode and lithium anode (theoretical capacity of 1675 mAh/g and 3840 mAh/g, respectively), the Li–S battery affords a high theoretical energy density and voltage platform. Therefore the battery can obtain a discharge capacity of 2–3 times larger than the commercial LIB and meet a driving range of over 500 km for electric vehicles (Fig. 7.2A) [23]. Moreover, the low cost of active materials provides Li–S batteries with economic and environmental advantages, making them extremely attractive for the energy storage fields [24].

Li–S battery consists of an electrode, electrolyte, and separator. Reaction intermediates polysulfides (Li_2S_x, $2 \leq x \leq 8$) exhibit high solubility in polar nonprotic media, while S_8 and Li_2S have low electron conductivity as electrode reaction materials [27]. During discharging, the sulfur molecule initially reacts with lithium ions to form polysulfide (Li_2S_x, $2 \leq x \leq 8$) and is converted into Li_2S at the end of complete discharge (Fig. 7.2B).

During the conversion from sulfur to Li_2S, the formation of the soluble polysulfide intermediate Li_2S_x ($2 \leq x \leq 8$) can attribute to a capacity of 418 mAh/g, while 1254 mAh/g is related to the Li_2S formation. The overall reaction is represented below [24]:

$$S_8 + 16Li^+ + 16e^- \leftrightarrow 8Li_2S$$

Although the Li–S battery reaction exhibits a 2-plateau discharge voltage curve, the actual battery reaction process is more complex. Therefore the cathode and anode of the battery still face several challenges.

Polysulfide shuttle effect. The solubility polysulfides (Li_2S_x, $4 \leq x \leq 8$) can diffuse to the anode to form insolubility polysulfides, which reduce the precipitation of Li_2S on the cathode surface at the end of discharge. The shuttle effect of polysulfides is essentially an internal short circuit that leads to the loss of active material (Fig. 7.2C) [25].

Low conductivity and large volumetric expansion. The electronic and ionic insulating properties of S_8 and Li_2S lead to low cathode utilization. During the discharging process, the generated Li_2S leads to the passivation of the cathode host, which limits the battery's capacity. In addition, the volume change of more than

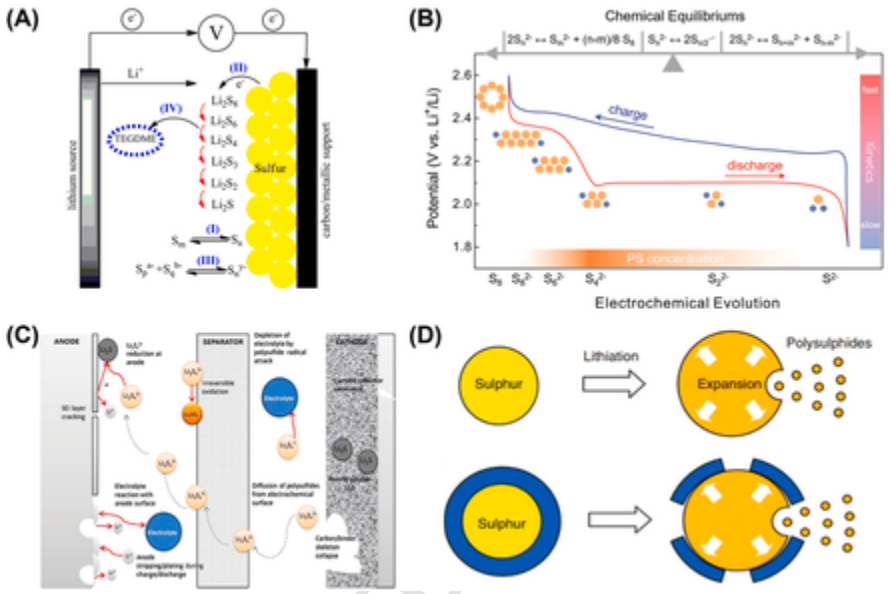

FIGURE 7.2

(A) Scheme of Li–S battery [23]. Copyright 2014, Reproduced with permission of American Chemical Society. (B) The compendium of polysulfide composition and evolution in Li–S battery [24]. Copyright 2018, Reproduced with permission of Wiley-VCH. (C) Summary of degradation mechanisms [25]. Copyright 2015, Reproduced with permission of Royal Society of Chemistry. (D) Schematic of the volumetric expansion and polysulfide dissolution process [26].

- Copyright 2013, Reproduced with permission of Nature Publishing Group.

80% for sulfur due to the density difference between S_8 and Li_2S (2.03 and 1.66 g/cm^3) can lead to fragmentation and structural cracking at the electrode level (Fig. 7.2D) [26].

Therefore nanoscale engineering has been widely investigated for high-performance Li–S systems to solve problems of the Li–S battery mentioned above.

7.2.1 Nanomaterials in the sulfur composite cathode

7.2.1.1 Carbon/sulfur composite cathode

To solve the problems of insulating sulfur, volume expansion, and the shuttle effect of polysulfides, carbon/sulfur composite cathodes have been developed. Different structured carbonaceous nanomaterials, for example, graphene [28], carbon nanotubes [29], mesoporous carbons [22], and hollow carbon nanospheres [30], with a high electric conductivity and porous structure, can serve as excellent cathode host.

Several studies have been reported that graphene oxide (GO) is a suitable host for sulfur accommodation. The presence of epoxy and hydroxyl groups in GO promotes the immobilization of sulfur, thus preventing its dissolution. Recently, graphene/sulfur composites as cathodes have been synthesized and tested in Li–S batteries. They exhibit better capacity, Coulombic efficiency, and cycling stability performance.

The graphene/sulfur composites have faster ion diffusion and higher electrical conductivity than the pure sulfur cathode. Qiu and coworkers reported a nanocomposite cathode that sulfur is wrapped inside the heteroatom-doped graphene host (NG). The X-ray spectroscopic analysis and DFT calculation imply the N functional groups in the NG host can form strong chemical bonds with polysulfides. Therefore with a 60 wt.% sulfur loading, the cathode could provide outstanding performance and an ultralow capacity decay rate[31].

The unique hollow nanostructures of CNTs make it easy to provide fast three-dimensional electron pathways and serve as a buffer zone for the sulfur host during the discharge/charge volume expansion. Ahn et al. synthesized a well-dispersed MWCNT/sulfur cathode by precipitation method, and sulfur was infiltrated into the hollow channel of MWCNTs [29]. The composite nanomaterial exhibited a high sulfur content of 80 wt.% with 1300 mAh/g specific capacity. However, a rather rapid decrease in capacity was obtained over 30 cycles, with 854 mAh/g observed. These results indicated a rather limited effect of pure CNTs for polysulfide trapping.

Although there has been extensive research on carbon materials as sulfur hosts, the synthesis costs still hinder the widespread use of graphene and CNTs in the cathode. Instead, low-cost biomass-derived porous carbon materials with moderate electronic conductivity are more practical as host materials. Ji and coworkers first encapsulated sulfur in ordered mesoporous carbon by a melting-diffusion method [22]. The composites could provide enough space to relieve the volume expansion of sulfur during charging/discharging, which obtained a high discharge capacity of over 1300 mAh/g. Based on this research, a series of porous carbon/sulfur nanocomposites have been studied to boost the performance of Li–S batteries [31–33].

7.2.1.2 Transition metal compounds/sulfur-composited cathodes

Nanostructured transition metal compounds (such as TiO_2, Co_3O_4, CoS_2, and MXene) have also been used as potential cathode host materials. Transition metal compounds facilitate polar polysulfide adsorption, resulting in the battery's high stability [34]. Moreover, transition metal compounds can improve cathode conductivity and enhance polysulfides' redox kinetically.

Transition metal oxides (TMOs) are unsuitable to be directly used as a sulfur host structure due to their poor porosity and sluggish electron and ion transport. Therefore varying TMO morphologies are generally used as composited cathodes

with other highly conductive nanomaterials (such as carbon materials, MXene, MOF, and conductive polymer) to increase cathode utilization.

Among TMOs, TiO_2 was the earliest studied cathode host material due to its controllable nanostructure and strong polarity. To inhibit the shuttle effect of polysulfide, a series of different structures of TiO_2 have been explored as cathode host materials, such as shells, nanotubes, and nanowires, or through their combination with tailored carbon structures. Cui et al. synthesized polar TiO_2 yolk shell nanostructure as cathode host material (Fig. 7.3A) [26]. The excellent capacity benefits from sufficient internal space to mitigate the volume expansion of the active material during cycling. Moreover, polar Ti-O groups and hydroxyl groups are regarded

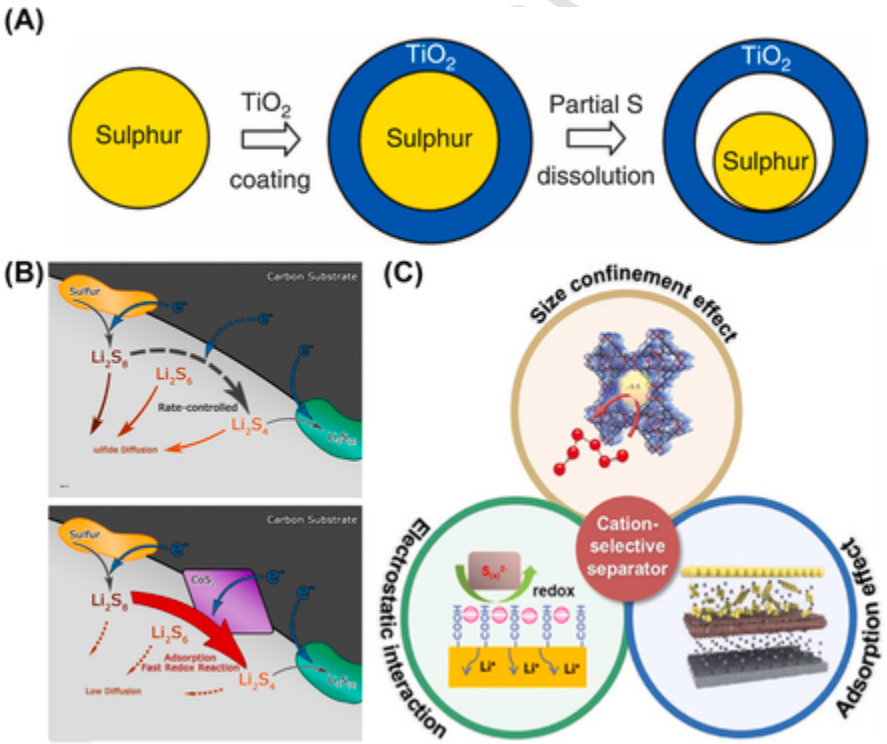

FIGURE 7.3

(A) Schematic illustration of S-TiO_2 nanostructures [26]. Copyright 2013, Reproduced with permission of Nature Publishing Group. (B) Schematic illustration of the difference in carbon/sulfur cathode and CoS_2-incorporated carbon/sulfur cathode during charging [36]. Copyright 2016, Reproduced with permission of American Chemical Society. (C) Strategies to address some issues of Li–S batteries by utilizing cation-selective separators regulating ionic transport [37].

to bind with polysulfides in minimizing polysulfide dissolution. The battery exhibits a high capacity of 1000 mAh/g and a low fade rate of 0.033% over 1000 cycles. However, sluggish electron transfer and poor electrical conductivity caused a fast capacity loss at a high rate. Therefore a heterostructure of TiO_2 (high absorptivity) and TiN (high electrical conductivity) was synthesized by Zhou and coworkers [35].

The heterostructure exerted a synergistic effect, allowing rapid diffusion of polysulfide to the conductive carbon surface while improving the deposition of Li_2S. The unique heterostructure achieves an initial discharge capacity of 927 mAh/g and an ultralow stable capacity retention of 73% during the 2000 cycles.

Transition metal sulfides (TMSs) act as a cathode host additive, with metal ions sulfur ions, providing a high valence electron density to the metal atoms, which creates binding sites for extrinsic sorbents polysulfides. For example, TiS_2 [38], CoS_2 [36], and Co_9S_8 [39] were added into Li_2S_6 solution to simulate the adsorption of Li–S battery intermediate of metal sulfide. The results showed that the electrolyte turned out to be clearly transparent, indicating the intermediate's excellent adsorption capacity. TMS can reduce the decomposition of batteries' polysulfide, boosting redox kinetics. Recently, nanoscale metal sulfides exhibited desirable electrochemical properties such as high capacity, cycling rates, and low redox potential. Zhang et al. successfully constructed the CoS_2/graphene composite cathodes to reduce charge transfer resistance, largely amplify electrochemical current response, and show strong chemical adsorption for polysulfides in Li–S batteries [36]. The nanoscale CoS_2/graphene cathode displayed a high discharge capacity and an ultralow decay rate during long-term cycling. As a mediator, CoS_2 promoted the conversion of the long-chain polysulfides to Li_2S and reduced the overpotential of Li_2S nucleation, while Li_2S was precipitated on conductive substrate graphene around CoS_2 (Fig. 7.3B).

7.2.2 Nanomaterials in the separator of Li–S batteries

The introduction of an ion-selective separator design was also proposed as an excellent strategy to promote good cycling stability and electrochemical reversibility of Li–S batteries. Advanced Li–S battery separators are designed to produce highly stable Li–S batteries by (1) restricting polysulfides diffusion to suppress shuttle effects, (2) reactivating accumulated dead active material species, and (3) limiting the growth of dendrites enrooting lithium anode (Fig. 7.3C) [37].

The bis((trifluoromethyl)sulfonyl)azanide (TFSI) anion in the electrolyte has a larger dynamic diameter (7.9 Å) compared to the Li^+ ion (~1.52 Å). Based on the sulfur and lithium radii and S-S bond length, the molecular size of polysulfide is estimated to be 14~25 Å, much larger than the Li–ion radius. Due to the difference in dynamic diameter between the anion and cation, it can selectively transport Li ions [37]. With a rational design of the pore size, the separator of the Li–S battery could be given the same function as the molecular sieve, the anions in the electrolyte would be kept on the cathode side of the separator, and Li^+ would be free shuttle on

both sides of separator. To construct an ion-selective separator based on the pore size effect, the separator modification materials are required to exhibit submicro/nanoporous structures, which include two-dimensional (2D) nanomaterials and metal-organic frameworks (MOFs). Wang et al. first proposed a 2D $Ti_3C_2T_x$-functionalized separator for anchoring polysulfides [40]. The Li–S battery with $Ti_3C_2T_x$-functionalized separator showed a discharge capacity of 550 mAh/g due to the balance of the blocking of polysulfides and improvement in electron conductivity. It exhibited a stable cycling performance and high retention at 0.5 C over 500 cycles.

7.3 Nanomaterials in metal–air batteries

The metal–air battery can realize the energy conversion between the chemical energy and the electricity by redox reaction operating on the electrodes. The performance of assembled battery involving rate ability, energy conversion efficiency, and cycling stability [41], is intensely correlated with the air electrode reaction of where the electrocatalytic oxygen reduction reaction (ORR) and oxygen evolution reaction (OER) [42]. It involves the oxygen redox reactions occurring in complex triple-phase interfaces (gaseous oxygen/liquid electrolyte/solid catalyst) [43]. Constructing the advanced air electrodes requires the catalysts to get the applicable kinetic reaction. Nanomaterials or nanostructures play vital effects in developing high-performance catalysts.

The ORR associated with air-cathode reactions should be described as the following steps [44–46]:

$$O_2 + 2H_2O + 4e^- \rightarrow 4OH^- \left[4e \text{ pathway}\right], \tag{7.1}$$

$$O_2 + H_2O + 2e^- \rightarrow HO_2^- + OH^- \left[2e \text{ pathway}\right], \tag{7.2}$$

The ORR could proceed through a four-electron (4e) route (7.1) or a two-electron (2e) route (7.2). Through the 4e pathway, the ORR owns the highest-energy conversion efficiency. However, the 2e pathway can produce the peroxide that causes the electrode to corrode to degrade battery performance.

The OER pathways are more complex. The elementary steps involve the adsorption of OH^- and O species on active sites (*) and as the reactions of (7.3) and (7.4) [47]:

$$OH^- + * \rightarrow OH^* + e^-, \tag{7.3}$$

$$OH^* + OH^- \rightarrow O* + H_2O + e^-, \tag{7.4}$$

The kinetics of oxygen reactions is intrinsically sluggish, which is the major obstacle to developing metal–air batteries. The nanomaterials in exploring the bifunctional catalysts toward ORR and OER are of great significance and have become the main approaches to improve the performance of metal–air batteries.

7.3.1 Noble metals and alloys catalysts

Platinum-group metals (PGMs) have been widely researched as the most active catalysts for the ORR, with remarkable electrochemical performance and high stability. Pt nanoparticles, atomic clusters, and single atoms uniformly distributed on the supports with a high surface area have been used as advanced ORR electrocatalysts. Pt catalysts own excellent catalytic activity and stability. However, high cost and scarcity seriously limit the applications of Pt catalysts. Therefore extensive efforts are paying to eliminate the high costs by finding the alternatives such as Pt alloys, nonnoble metals, or metal-free catalysts.

Pt-based alloys combing Pt metal with another metal are comparably active for ORR and OER with pure Pt. In Li–O_2 cells, the air electrode with PtAu/C catalyst exhibited the discharge and charge voltage close to Au/C and Pt/C [48] because Au and Pt atoms around the surface of catalysts can enhance the ORR and OER kinetics.

7.3.2 Transition metal compounds catalysts

Transition metal compounds, including oxides, sulfides, phosphides, and nitrides, have been explored as ORR/OER catalysts (Fig. 7.4) [49]. The intensive studies have pronounced that rock–salt-type monoxides such as CoO and NiO could significantly improve ORR/OER catalytic activities and perform comparably to the noble metal catalysts [50]. The representative spinel structure of Co_3O_4 and $NiCo_2O_4$ have been well demonstrated to simultaneously catalyze the ORR and OER due to their highly electrocatalytic activities.

TMSs have been promising as their good activity toward OER/ORR and simple preparation approaches. When it is in the oxidation process, the metal oxide/hydroxide species can be produced on the surface of TMS to contribute to the electrocatalytic activity of OER/ORR [51]. The recent results suggested that introducing the transition metal phosphide (TMP) into the TMS can chemically strengthen the bonding to improve the durability of the catalysts. The improved performance could arise from the 3p orbital lone pair electrons and free 3d orbitals of metal phosphorus [52]. Most transition metal compounds, including TMOs, hydro(oxy)oxides, and sulfides, are either insulators or semiconductors; intrinsically, as a consequence, considerable efforts have been devoted to solving the interfacial energy barriers due to the poor electron conductivity and the increased overpotential, which hampers energy conversion efficiency. The crucial challenges in boosting electrocatalysis performance are to accelerate electron transport.

In general, owing to the metallic electron transport behavior of transition metal nitrides (TMNs), it can accelerate the charge transfer between the catalysts and the supports. In addition, TMNs are interstitial compounds or alloys with a face-centered cubic arrangement of metal atoms. The introduction of nitride atoms into the parent metals can result into the expanding of lattice parameter. Since the good

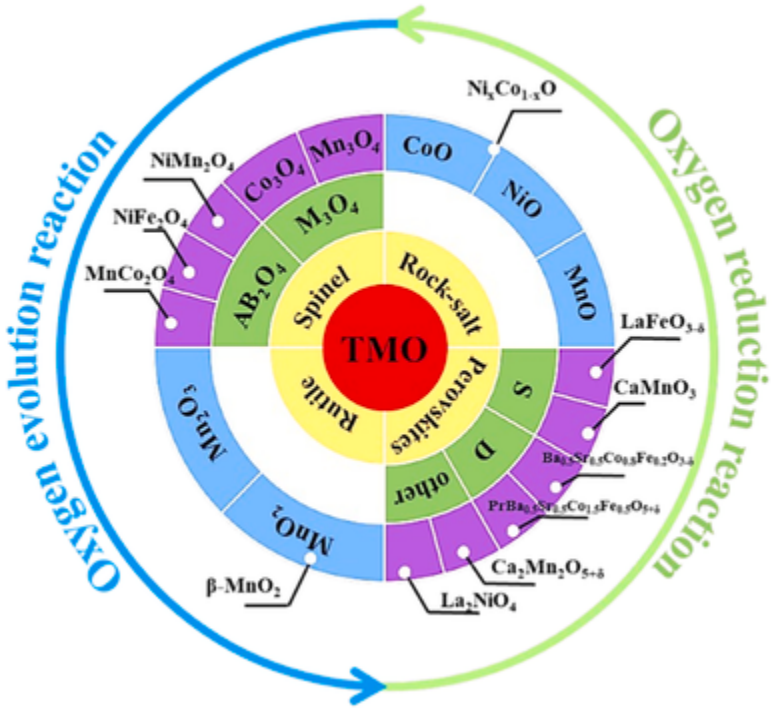

FIGURE 7.4

Schematic of intensely researched transition metal oxide catalysts for oxygen reduction reaction or oxygen evolution reaction [49].

- Copyright 2019, Reproduced with permission of the Royal Society of Chemistry.

ability arising from the intrinsic electron transport and the activity, it is promising to choose TMNs as electrocatalysts for metal–air batteries [53]. TMNs own a variety of valence states to supply the flexibility to tune electronic structure. Therefore some TMNs have been explored to be used as the bifunctional or even the multifunctional catalysts, which are beneficial to increase the specific energy of the rechargeable metal–air batteries [54]. Furthermore, TMNs have shown the high chemically and structurally durability during the ORR process.

7.3.3 Metal-free carbon-based catalysts

Carbon materials have excellent flexibility, high shape conformability, and electrical conductivity are considered commercially available substrate for the gas diffusion layers of metal–air batteries. Compared with conventional powdery counterparts, the self-supported carbon structure has many intrinsic advantages. The hydrophilic carbon supports can grow the catalysts directly to avoid the addition of

any ancillary additive, which exhibited high catalysis performance for the ORR and OER. The substrate materials can rivet and disperse catalysts, thus providing low interfacial contact resistance and high accessibility of multiphase active sites. In this regard, Liu's group [55] prepared a graphene containing rich edges and the oxygenated species on carbon cloth substrate (Fig. 7.5A). The obtained catalyst via in-situ Ar plasma treatment can be used as bifunctional OER/ORR electrode. Ma et al. reported a flexible self-supported g-C_3N_4 catalysts with phosphorus doping, which can reversibly catalyze ORR and OER [56]. Similarly, metal-free catalyst of the P-doped g-C_3N_4 growing on carbon fiber paper (PCN-CFP) with a large area (10 × 15 cm in size) and high flexibility (Fig. 7.5B), was fabricated, where P-doped g-C_3N_4 directly grew on the CFP to produce a flower-like porous frameworks (Fig. 7.5C). Dual doping of elementary N and P enabled the mass and charge transfer, the 3D CFP framework with a flower-like nanostructure enlarged the active surface areas. Therefore the PCN-CFP toward both ORR/OER exhibited the superior activity, stability, and reversibility over its powdery counterpart. The integrated electrodes are easier to realize accessibility of active sites and to decrease contact resistance without additional nonconductive binder. These advantages favor boosting performance of Zn–air batteries.

The defects in carbon materials could bring the electrolytic activity for ORR/OER, the electronic configuration modulation by tuning the defects in carbon can optimize the adsorption energy of intermediates during ORR/OER. Zhang and coworkers prepared the topological defects-enriched graphenes using the sticky rice and melamine as carbon precursors and MgO as templates. The experimental study and theoretical simulations consistently found that the adjacent defects of pentagon and heptagon (C5+C7) contribute to the prominent ORR and OER activity rather than N-doping sites [57] (Fig. 7.6A,B). Besides the defects formed around carbon materials, heteroatoms doping is a significant route to enable the catalytic activity of carbon materials, since it can efficiently tune the local electronic structure and

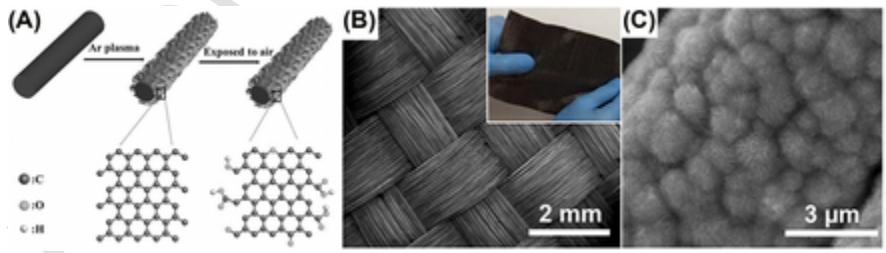

FIGURE 7.5

(A) In-situ exfoliation for preparation of the edge-rich and oxygen-functionalized graphene/carbon fiber electrode [55]. Copyright 2017, Reproduced with permission of John Wiley and Sons. (B, C) SEM images and (inset in panel A) photograph of P-doped g-C_3N_4 growing on CFP (PCN-CFP) [56].

- Copyright 2016, Reproduced with permission of Elsevier.

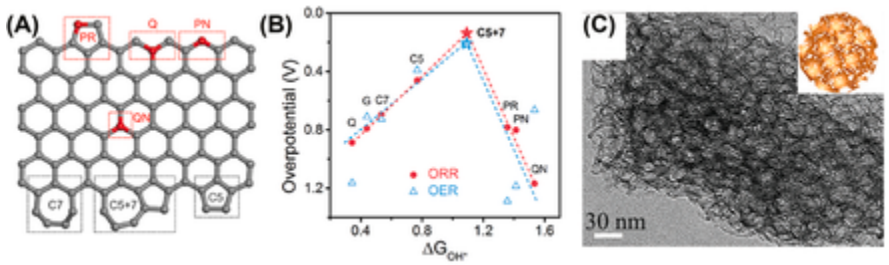

FIGURE 7.6

(A) Schematic illustration of graphene nanoribbon with different N-doped species or topological defects. (B) Volcano plots of ORR and OER overpotential concerning adsorption energy of OH* [57]. Copyright 2016, Reproduced with permission of John Wiley and Sons. (C) TEM images of N-doped porous carbon [59].

- Adapted with permission. Copyright 2018, Reproduced with permission of John Wiley and Sons.

the charge distribution of adjacent carbon atoms. Nitrogen atom is the extensively studied heteroatom dopant. For example, the optimized N-doped CNTs electrocatalyst was used as air-cathode supply the excellent power density of the Zn–air battery [58]. The hierarchically porous N-doped carbon can be produced by polymerizing o-phenylenediamine on silica template and the subsequent carbonization process and NH_3 etching processes (Fig. 7.6C). [59]. As a result, it exhibited an excellent ORR activity comparable with Pt/C. The metal-free carbon catalyst was obtained by assembling the N-doped graphene with the retained porosity and applied to Li–O_2 batteries [60]. The results demonstrated the superior electrocatalytic performances compared with the similar samples containing the TMOs or the precious metals.

7.4 Nanomaterials in all-solid-state batteries

Doping inorganic nanoparticles into polymer electrolyte systems is an approach widely used to optimize performance of solid electrolytes. The reasons of the excellent performance of polymer solid electrolytes with inorganic fillers are: (1) inorganic fillers can decrease the crystallinity of polymers to increase the amorphous phase region, which is benefited for Li^+ migration; (2) they increase fast ion transfer channels near the filler particles; (3) they can also improve the mechanical properties of polymer electrolytes. Inorganic fillers can be generally divided into inert materials, ionic conductor fillers, and electronic conductor fillers, among which inert fillers and ionic conductor fillers are the most studied.

7.4.1 Nano-inert materials in composite electrolytes

The inert filler mainly promotes the lithium salts dissociated and lowers the crystallinity of the polymer electrolytes through Lewis acid and alkali actions to improve the ionic conductivity, while it can also increase the thermal stability and the mechanical performance of electrolyte. Many types of inert materials including SiO_2 [61], Al_2O_3 [62], TiO_2 [63], ZrO_2 [64], etc., have been widely used to construct the composite solid electrolytes of inorganic–organic for solid-state lithium metal batteries, as shown in Fig. 7.7A. The inert nanofillers disarrange the polymer molecules structure to enhance the ionic conductivity of solid electrolyte at the room temperature. Lin et al. [65] filled the monodisperse 12 nm ultrafine SiO_2 in polyethylene oxide (PEO) through the hydrolysis of ethyl orthosilicate, and thus prepared the in-situ composite electrolyte PEO-SiO_2-$LiClO_4$. Chemical bonds and physical cross-link with PEO segments increase the amorphous region of PEO and raise the ionic conductivity at 30 °C to 4.4×10^{-5} S/cm.

In addition, montmorillonite is also one of the main research objects of solid electrolyte dopants. Doping a small amount of montmorillonite into the Poly(acrylonitrile) (PAN)-based membrane is beneficial to form continuous and stable Li–ions channels and increase ion mobility. He et al. [69] doped a small amount of organic montmorillonite (OMMT) into PAN-based electrolyte membrane to obtain hybrid solid-state electrolyte membrane. The first discharge specific capacity of solid LIB at 1 C is larger than pure PAN-based LIBs. The charge transfer resistance (R_{ct}) and the ion transfer resistance (R_{sei}) of OMMT-filled PAN become smaller than the corresponding PAN-based electrolyte membrane. Li et al. [70] reported the isocyanate-grafted Ti^{3+} doped TiO_2 using oxygen vacancies modified PEO electrolyte membrane. It was found that the oxygen vacancies in material enhance the interaction between the oxide surface and the anion groups of lithium salts, thereby changing the mobility of Li^+. Other oxides such as MgO and zeolite are often used as the inert fillers. The hybrid structure formed by the inactive materials filling polymers can achieve the ionic conductivity around the 10^{-5} S/cm at ambient temperature.

7.4.2 Nanoscale ionic conductors in composite electrolytes

Inorganic solid electrolytes are brittle and in weak contact with electrodes, resulting in high interfacial impedance. Therefore inorganic solid electrolyte systems are difficult to achieve practical applications. On the other hand, polymer electrolytes are easily deformed and have low ionic conductivity. It is generally believed that the two-phase interface between the inorganic active-filler and the polymer matrix has the higher ionic conductivity. Among the inorganic active-fillers, ionic conductivity types of garnet type (Garnet), perovskite type (Perovskite), NASICON type and sulfide are most widely studied [71].

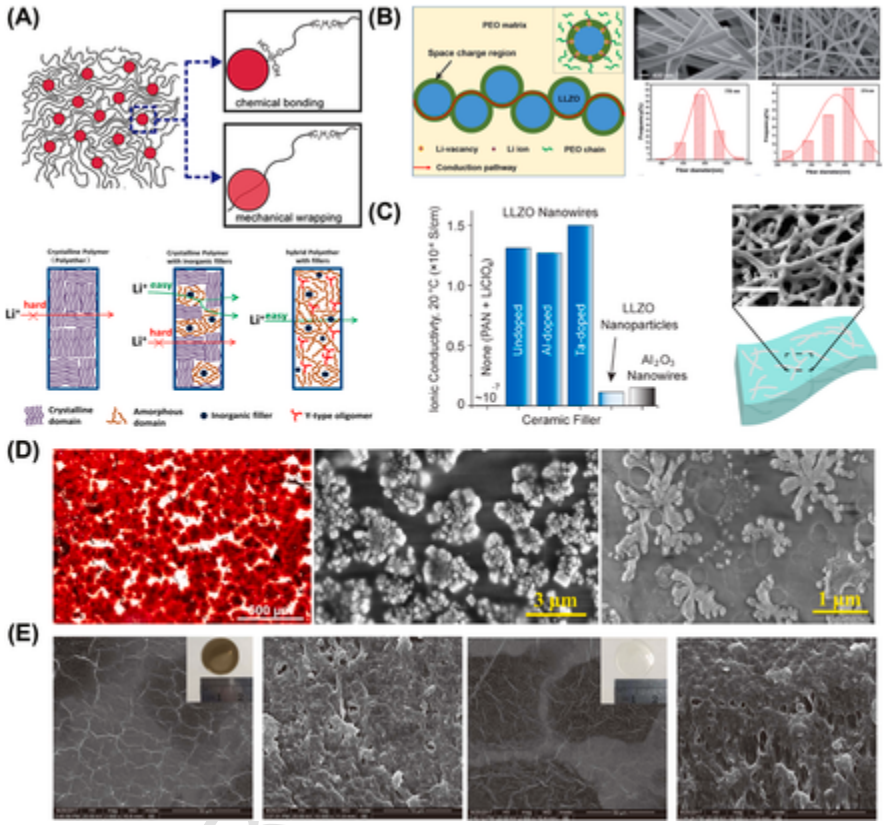

FIGURE 7.7

(A) Mechanism diagram of $MUSiO_2$ in-situ graft modification of PEO and the basic mechanisms of Li–ion transfer across different types of composite electrolytes [62,65]. Copyright 2022, Reproduced with permission of American Chemical Society, Copyright 2021, Reproduced with permission of Elsevier. (B) Schematic illustration of the ionic conduction pathway in different regions [66]. Copyright 2019, Reproduced with permission of American Chemical Society. (C) SEM images of electrospun LLZTO nanowires and physical properties [67]. Copyright 2019, Reproduced with permission of American Chemical Society. (D, E) Digital images and SEM images of the electrolyte surface [68].

- Copyright 2018, Reproduced with permission of Elsevier; Copyright 2021, Reproduced with permission of John Wiley and Sons.

Active-filler filled electrolyte has more complex and special ionic conductive behavior. First, active-filler itself can transport Li^+. Second, the two-phase interface formed by the active filler and the polymer has a space formed by the defect reaction of Li^+ migration to the crystal surface. The continuous space charge region is also the transport path of Li^+, as shown in Fig. 7.7B. Therefore active fillers can

significantly improve the ionic conductivity of solid electrolytes more than inert fillers.

Zhang et al. doped different proportions of $Li_{0.33}La_{0.57}TiO_3$ (LLTO) in the PEO electrolyte to increase its physical properties and ionic conductivity and withstand voltage stability window. Doping an appropriate proportion of nano-ceramic fillers with ionic conductivity in PEO can improve the performance of PEO-based solid electrolyte membrane, making it more stable and transporting more lithium ions compared with the solid polymer electrolyte without LLTO, the good dispersion of LLTO particles in the PEO matrix can generate Li–ion transfer channels near the particles to enhance the Li-ion transport [66,67]. Similarly, when 20 wt.% $Li_{6.75}La_3Zr_{1.75}Ta_{0.25}O_{12}$ (LLZTO) was introduced into PAN-based solid electrolyte, the obtained electrolyte exhibited the higher ionic conductivity, the withstand voltage stability window reached 4.9 V, suggesting that the doping of LLZTO can increase the Li^+ migration number and cycling stability of the solid electrolyte. LLZTO is also helpful in improving the interaction between the PAN matrix and lithium ions to increase the amount of dissolved lithium ions [72], as shown in Fig. 7.7C.

7.4.3 Nanometer electronic conductor in composite electrolytes

Electronic conductivity is generally minimized as an electrolyte since most attention has been focused on improving solid electrolyte ion transfer rate. Therefore the application of electronic conductors in solid electrolytes is considerably rare. In several recent years, it was discovered that in-situ modification of the electrode–electrolyte interface with electron conductors to ensure electron homogeneity at the electrode–electrolyte interface could achieve good interfacial contact and long-lasting battery cycles.

Zheng et al. [68] designed the in-situ growth of nano-sized "flower"-like conductive polythiophene particles at the electrode–electrolyte interface, intertwined with PEO to form a mixed ion–electron transfer interface layer (Fig. 7.7D). Coincidentally, as an electronic nanofiller, the GOs were added into Solid Polymer Electrolytes (SPEs) at different ratios. When the GO content is 1.0 wt.%, the ionic conductivity of the composite electrolyte is raised to 4.0×10^{-4} S/cm (Fig. 7.7E).

7.5 Summary and outlook

With the market needs for long-range electric automobiles and large-scale energy storage stations, high-energy-density batteries have been attracted more attention. Nanomaterials and nanotechnologies have significantly affected the development of electrode materials for conventional LIBs and new battery systems with potential applications (Li–S batteries, metal–air batteries, and all-solid-state batteries).

LIBs face many challenges, such as side reactions, slow kinetic rates, structural damage, and unstable surface Solid Electrolyte Interphase (SEI), which will affect the ability of electrode materials from electronic conductivity, and Li^+ diffusivity to

obtain the optimal electrochemical performance. Li–S batteries encountered the polysulfide shuttle effect, low conductivity, and large volumetric expansion. The novel material/active material holding sulfur, nanotechnology on the electrode, design of multifunctional separators, and the fundamental reaction mechanism have been widely concerned. The precious catalysts with high-cost and scarcity for metal–air batteries have seriously limited their applications. Designing and developing nonnoble metal catalysts with high activity by nanotechnologies have been demonstrated as effective means to boost the ORR/OER of metal–air batteries. Solid electrolytes are critical in the development of all solid batteries. To enhance the ion conductivity and to improve the mechanical stability of solid electrolytes, the application of inert and active nanomaterials in the solid electrolytes can improve the charge-discharge, rate, and stability performance of all-solid-state batteries.

Here, we briefly overviewed and discussed nanomaterials' advantages in solving the above problems. Meanwhile, the challenges such as the high-cost and complex multistep processing by utilizing nanomaterials in batteries have to be considered. Exploring novel nanomaterials, designing rational nanostructure, and getting good compatibility with electrode materials would be the possible routes to apply nanomaterials in batteries shortly.

References

[1] H. Li, H.J. Zhou, Enhancing the performances of Li-ion batteries by carbon-coating: present and future, Chem. Commun. 48 (9) (2012) 1201–1217. https://doi.org/10.1039/C1CC14764A.

[2] J. Gao, L. Fu, H. Zhang, T. Zhang, Y. Wu, H.J. Wu, Suppression of PC decomposition at the surface of graphitic carbon by Cu coating, Electrochem. Commun. 8 (11) (2006) 1726–1730. https://doi.org/10.1016/j.elecom.2006.08.011.

[3] L. Yang, W. Guo, Y. Shi, Y.J. Wu, Graphite@MoO_3 composite as anode material for lithium ion battery in propylene carbonate-based electrolyte, J. Alloys Compd. 501 (2) (2010) 218–220. https://doi.org/10.1016/j.jallcom.2009.11.196.

[4] W. Lu, V. Donepudi, J. Prakash, J. Liu, K.J. Amine, Electrochemical and thermal behavior of copper coated type MAG-20 natural graphite, Electrochim. Acta 47 (10) (2002) 1601–1606. https://doi.org/10.1016/S0013-4686(01)00883-0.

[5] Y.K. Sun, M.J. Lee, C.S. Yoon, J. Hassoun, K. Amine, B.J. Scrosati, The role of AlF_3 coatings in improving electrochemical cycling of Li-enriched nickel-manganese oxide electrodes for Li-ion batteries, Adv. Mater. 24 (9) (2012) 1192–1196. https://doi.org/10.1002/adma.201104106.

[6] R. Chebiam, A. Kannan, F. Prado, A.J. Manthiram, Comparison of the chemical stability of the high energy density cathodes of lithium-ion batteries, Electrochem. Commun. 3 (11) (2001) 624–627. https://doi.org/10.1016/S1388-2481(01)00232-6.

[7] L. Liu, X.J. Chen, Titanium dioxide nanomaterials: self-structural modifications, Chem. Rev. 114 (19) (2014) 9890–9918. https://doi.org/10.1021/cr400624r.

[8] Y.K. Sun, Z. Chen, H.J. Noh, D.J. Lee, H.G. Jung, Y. Ren, et al., Nanostructured high-energy cathode materials for advanced lithium batteries, Nat. Mater. 11 (11) (2012) 942–947. https://doi.org/10.1038/NMAT3435.

[9] P. Zhang, D. Zhang, L. Huang, Q. Wei, M. Lin, X.J. Ren, First-principles study on the

electronic structure of a $LiFePO_4$ (0 1 0) surface adsorbed with carbon, J. Alloys Compd. 540 (2012) 121–126. https://doi.org/10.1016/j.jallcom.2012.06.049.

[10] A.F. Gonzalez, N.H. Yang, R.S. Liu, Silicon anode design for lithium-ion batteries: progress and perspectives, J. Phys. Chem. C. 121 (2017) 27775–277787. https://doi.org/10.1021/acs.jpcc.7b07793.

[11] X.H. Liu, J.Y. Huang, In situ TEM electrochemistry of anode materials in lithium ion batteries, Energy Environ. Sci. 4 (10) (2011) 3844–3860. https://doi.org/10.1039/C1EE01918J.

[12] B. Wang, X. Li, X. Zhang, B. Luo, M. Jin, M. Liang, et al., Adaptable silicon-carbon nanocables sandwiched between reduced graphene oxide sheets as lithium-ion battery anodes, ACS Nano 7 (2) (2013) 1437–1445. https://doi.org/10.1021/nn3052023.

[13] T. Song, J. Xia, J.H. Lee, D.H. Lee, M.S. Kwon, J.M. Choi, et al., Arrays of sealed silicon nanotubes as anodes for lithium ion batteries, Nano Lett. 10 (5) (2010) 1710–1716. https://doi.org/10.1021/nl100086e.

[14] T. Yang, S. Li, W. Wang, J. Lu, W. Fan, X. Zuo, et al., Nonflammable functional electrolytes with all-fluorinated solvents matching rechargeable high-voltage Li-metal batteries with Ni-rich ternary cathode, J. Power Sources 505 (2021) 230055–230066. https://doi.org/10.1016/j.jpowsour.2021.230055.

[15] M.Z. Kufian, S. Ramesh, A.J. Arof, PMMA-LiTFSI based gel polymer electrolyte for lithium-oxygen cell application, Opt. Mater. 120 (2021) 111418–111428. https://doi.org/10.1016/j.optmat.2021.111418.

[16] H. Zhang, X. Liao, Y. Guan, Y. Xiang, M. Li, W. Zhang, et al., Lithiophilic-lithiophobic gradient interfacial layer for a highly stable lithium metal anode, Nat. Commun. 9 (1) (2018) 1–11. https://doi.org/10.1038/s41467-018-06126-z.

[17] H. Wu, G. Chan, J.W. Choi, I. Ryu, Y. Yao, M.T. McDowell, et al., Stable cycling of double-walled silicon nanotube battery anodes through solid–electrolyte interphase control, Nat. Nanotechnol. 7 (5) (2012) 310–315. https://doi.org/10.1038/NNANO.2012.35.

[18] G. Hu, R. Yu, Z. Liu, Q. Yu, Y. Zhang, Q. Chen, et al., Surface oxidation layer-mediated conformal carbon coating on Si nanoparticles for enhanced lithium storage, ACS Appl. Mater. Interface 13 (3) (2021) 3991–3998. https://doi.org/10.1021/acsami.0c19673.

[19] S. Fang, L. Shen, G. Xu, P. Nie, J. Wang, H. Dou, et al., Rational design of void-involved $Si@TiO_2$ nanospheres as high-performance anode material for lithium-ion batteries, ACS Appl. Mater. Interface 6 (9) (2014) 6497–6503. https://doi.org/10.1021/am500066j.

[20] D.T. Ngo, H.T. Le, X.M. Pham, C.N. Park, C.J. Park, Facile synthesis of Si@SiC composite as an anode material for lithium-ion batteries, ACS Appl. Mater. Interface 9 (38) (2017) 32790–32800. https://doi.org/10.1021/acsami.7b10658.

[21] Y. Yu, G. Li, X. Chen, W. Lin, J. Rong, W.J. Yang, Rigid TiO_{2-x} coated mesoporous hollow Si nanospheres with high structure stability for lithium-ion battery anodes, RSC Adv. 8 (27) (2018) 15094–15101. https://doi.org/10.1039/C8RA01661E.

[22] X. Ji, K.T. Lee, L.F. Nazar, A highly ordered nanostructured carbon-sulphur cathode for lithium-sulphur batteries, Nat. Mater. 8 (6) (2009) 500–506. https://doi.org/10.1038/nmat2460.

[23] R.S. Assary, L.A. Curtiss, J.S. Moore, Toward a molecular understanding of energetics in Li–S batteries using nonaqueous electrolytes: a high-level quantum chemical study, The J. Phys. Chem. C 118 (22) (2014) 11545–11558.

[24] G. Li, S. Wang, Y. Zhang, M. Li, Z. Chen, J. Lu, Revisiting the role of polysulfides in lithium–sulfur batteries, Adv. Mater. 30 (22) (2018) 1705590.
[25] M. Wild, L. O'Neill, T. Zhang, R. Purkayastha, M. Marinescu, G.J. Offer, Lithium sulfur batteries, a mechanistic review, Energy & Environ. Sci. 8 (12) (2015) 3477–3494.
[26] Z.W. Seh, W. Li, J.J. Cha, G. Zheng, Y. Yang, M.T. McDowell, et al., Sulphur-TiO_2 yolk-shell nanoarchitecture with internal void space for long-cycle lithium-sulphur batteries, Nat. Commun. 4 (2013) 1331–1336. https://doi.org/10.1038/ncomms2327.
[27] A. Manthiram, Y. Fu, Y.S. Su, Challenges and prospects of lithium-sulfur batteries, Acc. Chem. Res. 46 (5) (2013) 1125–1134. https://doi.org/10.1021/ar300179v.
[28] J.Z. Wang, L. Lu, M. Choucair, J.A. Stride, X. Xu, H.K. Liu, Sulfur-graphene composite for rechargeable lithium batteries, J. Power Sources 196 (16) (2011) 7030–7034. https://doi.org/10.1016/j.jpowsour.2010.09.106.
[29] W. Ahn, K.B. Kim, K.N. Jung, K.H. Shin, C.S. Jin, Synthesis and electrochemical properties of a sulfur-multi walled carbon nanotubes composite as a cathode material for lithium sulfur batteries, J. Power Sources 202 (2012) 394–399. https://doi.org/10.1016/j.jpowsour.2011.11.074.
[30] G. He, S. Evers, X. Liang, M. Cuisinier, A. Garsuch, L.F. Nazar, Tailoring porosity in carbon nanospheres for lithium-sulfur battery cathodes, ACS Nano 7 (12) (2013) 10920–10930. https://doi.org/10.1021/nn404439r.
[31] Z. Wang, Y. Dong, H. Li, et al., Enhancing lithium-sulphur battery perormance by stronglybinding the discharge products oene oxidelJ.Naturen amino-functionalized reduced graphene oxiede, Nat. Commun. 5 (1) (2014) 5002.
[32] H. Zhang, Z. Zhao, Y. Liu, J. Liang, Y. Hou, Z. Zhang, et al., Nitrogen-doped hierarchical porous carbon derived from metal-organic aerogel for high performance lithium–sulfur batteries, J. Energy Chem. 26 (6) (2017) 1282–1290. https://doi.org/10.1016/j.jechem.2017.08.016.
[33] Z. Zhang, Z. Li, F. Hao, X. Wang, Q. Li, Y. Qi, et al., 3D interconnected porous carbon aerogels as sulfur immobilizers for sulfur impregnation for lithium-sulfur batteries with high rate capability and cycling stability, Adv. Funct. Mater. 24 (17) (2014) 2500–2509. https://doi.org/10.1002/adfm.201303080.
[34] X. Liu, J.Q. Huang, Q. Zhang, L. Mai, Nanostructured metal oxides and sulfides for lithium-sulfur batteries, Adv. Mater. 29 (20) (2017) 1601759–1601783. https://doi.org/10.1002/adma.201601759.
[35] T. Zhou, W. Lv, J. Li, G. Zhou, Y. Zhao, S. Fan, B. Liu, B. Li, F. Kang, Q. H. Yang, Twinborn TiO_2-TiN heterostructures enabling smooth trapping-diffusion-conversion of polysulfides towards ultralong life lithium–sulfur batteries, Energy Environ. Sci. 10 (7) (2017) 1694–1703.
[36] Z. Yuan, H.J. Peng, T.Z. Hou, J.Q. Huang, C.M. Chen, D.W. Wang, X.B. Cheng, F. Wei, Q. Zhang, Powering lithium-sulfur battery performance by propelling polysulfide redox at sulfiphilic hosts, Nano Lett. 16 (1) (2016) 519–527.
[37] Q. Zhao, Z. Hao, J. Tang, X. Xu, J. Liu,, Y. Jin, Q. Zhang, H. Wang, Cation-selective separators for addressing the lithium-sulfur battery challenges, ChemSusChem 14 (3) (2021) 792–807.
[38] X. Huang, J. Tang, B. Luo, R. Knibbe, T. Lin, H. Hu, M. Rana, Y. Hu, X. Zhu, Q. Gu, D. Wang, L. Wang, Sandwich-like ultrathin TiS_2 nanosheets confined within N, S codoped porous carbon as an effective polysulfide promoter in lithium-sulfur batteries, Adv. Energy Mater. 9 (32) (2019) 1901872–1901880.

[39] Q. Pang, D. Kundu, L.F. Nazar, A graphene-like metallic cathode host for long-life and high-loading lithium–sulfur batteries, Mater. Horiz. 3 (2) (2016) 130–136.
[40] J. Song, D. Su, X. Xie, X. Guo, W. Bao, G. Shao, et al., Immobilizing polysulfides with MXene-functionalized separators for stable lithium-sulfur batteries,, ACS Appl. Mater. Interface 8 (43) (2016) 29427–29433. https://doi.org/10.1021/acsami.6b09027.
[41] R. Cao, J.S. Lee, M. Liu, J. Cho, Recent progress in non-precious catalysts for metal-air batteries, Adv. Energy Mater. 2 (7) (2012) 816–829. https://doi.org/10.1002/aenm.201200013.
[42] V. Neburchilov, H. Wang, J.J. Martin, W. Qu, A review on air cathodes for zinc–air fuel cells, J. Power Sources 195 (5) (2010) 1271–1291. https://doi.org/10.1016/j.jpowsour.2009.08.100.
[43] G. Liu, W.S.Y. Wong, M. Kraft, J.W. Ager, D. Vollmerc, R. Xu,, Wetting-regulated gas-involving (photo) electrocatalysis: biomimetics in energy conversion, Chem. Soc. Rev. 50 (18) (2021) 10674–10699. https://doi.org/10.1039/D1CS00258A.
[44] J.S. Spendelow, A. Wieckowski, Electrocatalysis of oxygen reduction and small alcohol oxidation in alkaline media, Phys. Chem. Chem. Phys. 9 (21) (2007) 2654–2675. https://doi.org/10.1039/B703315J.
[45] P. Christensen, A. Hamnett, D. Linares-Moya, Oxygen reduction and fuel oxidation in alkaline solution, Phys. Chem. Chem. Phys. 13 (12) (2011) 5206–5214. https://doi.org/10.1039/C0CP02365E.
[46] F. Cheng, J. Chen, Metal-air batteries: from oxygen reduction electrochemistry to cathode catalysts, Chem. Soc. Rev. 41 (6) (2012) 2172–2192. https://doi.org/10.1039/c1cs15228a.
[47] M. Bajdich, M. García-Mota, A. Vojvodic, J.K. Nørskov, A.T. Bell, Theoretical investigation of the activity of cobalt oxides for the electrochemical oxidation of water, J. Am. Chem. Soc. 135 (36) (2013) 13521–13530. https://doi.org/10.1021/ja405997s.
[48] Y.C. Lu, Z. Xu, H.A. Gasteiger, S. Chen, K. Hamad-Schifferli, Y.S. Horn, Platinum-gold nanoparticles: a highly active bifunctional electrocatalyst for rechargeable lithium-air batteries, J. Am. Chem. Soc. 132 (35) (2010) 12170–12171. https://doi.org/10.1021/ja1036572.
[49] Y. Zhu, X. Liu, S. Jin, H. Chen, W. Lee, M. Liu, et al., Anionic defect engineering of transition metal oxides for oxygen reduction and evolution reactions, J. Mater. Chem. A 7 (11) (2019) 5875–5897. https://doi.org/10.1039/c8ta12477a.
[50] T. Zhang, M.Y. Wu, D.Y. Yan, J. Mao, H. Liu, W.B. Hu, et al., Engineering oxygen vacancy on NiO nanorod arrays for alkaline hydrogen evolution, Nano Energy 43 (2018) 103–109. https://doi.org/10.1016/j.nanoen.2017.11.015.
[51] S. Jin, Are metal chalcogenides, nitrides, and phosphides oxygen evolution catalysts or bifunctional catalysts?, ACS Energy Lett. 2 (2017) 1937–1938. https://doi.org/10.1021/acsenergylett.7b00679.
[52] D.S. Yang, D. Bhattacharjya, S. Inamdar, J. Park, J.S. Yu, Phosphorus-doped ordered mesoporous carbons with different lengths as efficient metal-free electrocatalysts for oxygen reduction reaction in alkaline media, J. Am. Chem. Soc. 134 (39) (2012) 16127–16130. https://doi.org/10.1021/ja306376s.
[53] X. Yu, T. Zhou, J. Ge, C. Wu, Recent advances on the modulation of electrocatalysts based on transition metal nitrides for the rechargeable Zn-air battery, ACS Mater. Lett. 2 (11) (2020) 1423–1434. https://doi.org/10.1021/acsmaterialslett.0c00339.
[54] J. Luo, X. Qiao, J. Jin, X. Tian, H. Fan, D. Yu, et al., A strategy to unlock the potential of CrN as a highly active oxygen reduction reaction catalyst, J. Mater. Chem. A 8 (17)

(2020) 8575–8585. https://doi.org/10.1039/c9ta14085a.
[55] Z. Liu, Z. Zhao, Y. Wang, S. Dou, D. Yan, D. Liu, et al., In situ exfoliated, edge-rich, oxygen-functionalized graphene from carbon fibers for oxygen electrocatalysis, Adv. Mater. 29 (18) (2017) 1606207–1606213. https://doi.org/10.1002/adma.201606207.
[56] T.Y. Ma, S. Dai, S.Z. Qiao, Self-supported electrocatalysts for advanced energy conversion processes, Mater. Today 19 (5) (2016) 265–273. https://doi.org/10.1016/j.mattod.2015.10.012.
[57] C. Tang, H.F. Wang, X. Chen, B.Q. Li, T.Z. Hou, B. Zhang, et al., Topological defects in metal-free nanocarbon for oxygen electrocatalysis, Adv. Mater. 28 (32) (2016) 6845–6851. https://doi.org/10.1002/adma.201601406.
[58] S. Zhu, Z. Chen, B. Li, D. Higgins, H. Wang, H. Li, et al., Nitrogen-doped carbon nanotubes as air cathode catalysts in zinc-air battery, Electrochim. Acta 56 (14) (2011) 5080–5084. https://doi.org/10.1016/j.electacta.2011.03.082.
[59] J. Pan, Y.Y. Xu, H. Yang, Z. Dong, H. Liu, B.Y. Xia, Advanced architectures and relatives of air electrodes in Zn-air batteries, Adv. Sci. 5 (4) (2018) 1700691–1700720. https://doi.org/10.1002/advs.201700691.
[60] J. Shui, Y. Lin, J.W. Connell, J. Xu, X. Fan, L. Dai, Nitrogen-doped holey graphene for high-performance rechargeable Li-O_2 batteries, ACS Energy Lett. 1 (1) (2016) 260–265. https://doi.org/10.1021/acsenergylett.6b00128.
[61] C.W. Nan, L. Fan, Y. Lin, Q. Cai, Enhanced ionic conductivity of polymer electrolytes containing nanocomposite SiO_2 particles, Phys. Rev. Lett. 91 (26) (2003) 266104–266107. https://doi.org/10.1103/PhysRevLett.91.266104.
[62] R. Tan, R. Gao, Y. Zhao, M. Zhang, J. Xu, J. Yang, et al., Novel organic-inorganic hybrid electrolyte to enable $LiFePO_4$ quasi-solid-state Li-ion batteries performed highly around room temperature, ACS Appl. Mater. Interface 8 (2016) 31273–31280. https://doi.org/10.1021/acsami.6b09008.
[63] S. Hua, J. Li, M. Jing, F. Chen, B. Ju, F. Tu, et al., Effects of surface lithiated TiO_2 nanorods on room-temperature properties of polymer solid electrolytes, Int. J. Energy Res. 44 (8) (2020) 6452–6462. https://doi.org/10.1002/er.5379.
[64] G. Derrien, J. Hassoun, S. Sacchetti, S. Panero, Nanocomposite PEO-based polymer electrolyte using a highly porous, super acid zirconia filler, Solid. State Ion. 180 (23–25) (2009) 1267–1271. https://doi.org/10.1016/j.ssi.2009.07.006.
[65] D. Lin, W. Liu, Y. Liu, H.R. Lee, P.C. Hsu, K. Liu, et al., High ionic conductivity of composite solid polymer electrolyte via in situ synthesis of monodispersed SiO_2 nanospheres in poly (ethylene oxide), Nano Lett. 16 (1) (2016) 459–465. https://doi.org/10.1021/acs.nanolett.5b04117.
[66] P. Zhu, C. Yan, M. Dirican, J. Zhu, J. Zang, R.K. Selvan, et al., $Li_{0.33}La_{0.557}TiO_3$ ceramic nanofiber-enhanced polyethylene oxide-based composite polymer electrolytes for all-solid-state lithium batteries, J. Mater. Chem. A 6 (10) (2018) 4279–4285. https://doi.org/10.1039/C7TA10517G.
[67] T. Yang, J. Zheng, Q. Cheng, Y.Y. Hu, C.K. Chan, Composite polymer electrolytes with $Li_7La_3Zr_2O_{12}$ garnet-type nanowires as ceramic fillers: mechanism of conductivity enhancement and role of doping and morphology, ACS Appl. Mater. Interface 9 (26) (2017) 21773–21780. https://doi.org/10.1021/acsami.7b03806.
[68] J. Zheng, C. Sun, Z. Wang, S. Liu, B. An, Z. Sun, et al., Double ionic-electronic transfer interface layers for all-solid-state lithium batteries, Angew. Chem. Int. Edit. 60 (34) (2021) 18448–18453. https://doi.org/10.1002/anie.202104183.
[69] C. He, J. Liu, J. Cui, J. Li, X. Wu, A gel polymer electrolyte based on polyacrylonitrile/

organic montmorillonite membrane exhibiting dense structure for lithium ion battery, Solid. State Ion. 315 (2018) 102–110. https://doi.org/10.1016/j.ssi.2017.12.014.

[70] C. Li, Y. Huang, C. Chen, X. Feng, Z. Zhang, High-performance polymer electrolyte membrane modified with isocyanate-grafted Ti^{3+} doped TiO_2 nanowires for lithium batteries, Appl. Surf. Sci. 563 (2021) 150248–150256. https://doi.org/10.1016/j.apsusc.2021.150248.

[71] G. Xi, M. Xiao, S. Wang, D. Han, Y. Li, Y. Meng, Polymer-based solid electrolytes: material selection, design, and application, Adv. Funct. Mater. 31 (9) (2020) 2007598–2007625. https://doi.org/10.1002/adfm.202007598.

[72] X. Zhang, B.Q. Xu, Y.H. Lin, Y. Shen, L. Li, C.W. Nan, Effects of $Li_{6.75}La_3Zr_{1.75}Ta_{0.25}O_{12}$ on chemical and electrochemical properties of polyacrylonitrile-based solid electrolytes, Solid. State Ion. 327 (2018) 32–38. https://doi.org/10.1016/j.ssi.2018.10.023.